Mice surgery and treatment

We obtained 6-week-old R62 transgenic mice and CBA × C57Bl/6 F_1 wild-type littermates from Jackson laboratories. The genotype was confirmed by polymerase chain reaction as described[7]. Mice were treated after 1 week of daily rotarod training. Mice were anaesthetized by intraperitoneal injection of chloral hydrate and osmotic pumps (0.25 μl h^{-1} for 28 d), and the cannula were implanted intracerebroventricularly (Alzet) using predetermined coordinates (anterior/posterior, −0.5 mm, 1 mm lateral to the bregma). Congo red was diluted at 1 mg ml^{-1} in calcium- and magnesium-free PBS plus 0.2% DMSO. The vehicle solution contained 0.2% DMSO in calcium- and magnesium-free PBS. For intraperitoneal injections, 0.5 ml of 1 mg ml^{-1} Congo red in PBS plus 0.2% DMSO was injected every 48 h. The protocol was approved by the Harvard Medical School Standing Committee on Animals.

Behavioural tests, rotarod performance

Two days after their first treatment, we tested the mice for motor performance and coordination by using a rotarod (Columbus Instruments) at 10 r.p.m. for a maximum of 210 s and by the 'ink' test[30]. The mice were weighed once a week. Two rotarod trials were carried out three times a week in a blind manner.

Tissue preparation and histology

Mice were anaesthetized with isoflurane and perfused intracardially with 4% paraformaldehyde in PBS. The brain was removed and washed several times in PBS before being incubated overnight in PBS containing 30% sucrose and embedded in OCT (optimal culling temperature) (Sigma) for sectioning. We stained the sections with EM48 antibodies at a dilution of 1:1,000 and detected immunoreactivity with the ABC kit according to the manufacturer's instructions (Vector).

Received 14 August; accepted 6 November 2002; doi:10.1038/nature01301.

1. The Huntington's Disease Collaborative Research Group. A novel gene containing a trinucleotide repeat that is expanded and unstable on Huntington's disease chromosomes. *Cell* **72,** 971–983 (1993).
2. Wellington, C. L. *et al.* Inhibiting caspase cleavage of huntingtin reduces toxicity and aggregate formation in neuronal and nonneuronal cells. *J. Biol. Chem.* **275,** 19831–19838 (2000).
3. Kim, Y. J. *et al.* Caspase 3-cleaved N-terminal fragments of wild-type and mutant huntingtin are present in normal and Huntington's disease brains, associate with membranes, and undergo calpain-dependent proteolysis. *Proc. Natl Acad. Sci. USA* **98,** 12784–12789 (2001).
4. Lunkes, A. *et al.* Proteases acting on mutant huntingtin generate cleaved products that differentially build up cytoplasmic and nuclear inclusions. *Mol. Cell* **10,** 259–269 (2002).
5. Wellington, C. L. *et al.* Caspase cleavage of mutant huntingtin precedes neurodegeneration in Huntington's disease. *J. Neurosci.* **22,** 7862–7872 (2002).
6. Perutz, M. Polar zippers: their role in human disease. *Protein Sci.* **3,** 1629–1637 (1994).
7. Mangiarini, L. *et al.* Exon 1 of the HD gene with an expanded CAG repeat is sufficient to cause a progressive neurological phenotype in transgenic mice. *Cell* **87,** 493–506 (1996).
8. Klunk, W. E., Pettegrew, J. W. & Abraham, D. J. Quantitative evaluation of Congo red binding to amyloid-like proteins with a β-pleated sheet conformation. *J. Histochem. Cytochem.* **37,** 1273–1281 (1989).
9. Carter, D. B. & Chou, K. C. A model for structure-dependent binding of Congo red to Alzheimer β-amyloid fibrils. *Neurobiol. Aging* **19,** 37–40 (1998).
10. Heiser, V. *et al.* Inhibition of huntingtin fibrillogenesis by specific antibodies and small molecules: implications for Huntington's disease therapy. *Proc. Natl Acad. Sci. USA* **97,** 6739–6744 (2000).
11. Caughey, B. & Raymond, G. J. Sulfated polyanion inhibition of scrapie-associated PrP accumulation in cultured cells. *J. Virol.* **67,** 643–650 (1993).
12. Howlett, D. R., George, A. R., Owen, D. E., Ward, R. V. & Markwell, R. E. Common structural features determine the effectiveness of carvedilol, daunomycin and rolitetracycline as inhibitors of Alzheimer β-amyloid fibril formation. *Biochem. J.* **343,** 419–423 (1999).
13. Klunk, W. E., Debnath, M. L. & Pettegrew, J. W. Chrysamine-G binding to Alzheimer and control brain: autopsy study of a new amyloid probe. *Neurobiol. Aging* **16,** 541–548 (1995).
14. Sanchez, I. *et al.* Caspase-8 is required for cell death induced by expanded polyglutamine repeats. *Neuron* **22,** 623–633 (1999).
15. Beal, M. F., Hyman, B. T. & Koroshetz, W. Do defects in mitochondrial energy metabolism underlie the pathology of neurodegenerative diseases? *Trends Neurosci.* **16,** 125–131 (1993).
16. Deckwerth, T. L. & Johnson, E. M. Jr Temporal analysis of events associated with programmed cell death (apoptosis) of sympathetic neurons deprived of nerve growth factor. *J. Cell Biol.* **123,** 1207–1222 (1993).
17. Jaattela, M., Wissing, D., Kokholm, K., Kallunki, T. & Egeblad, M. Hsp70 exerts its anti-apoptotic function downstream of caspase-3-like proteases. *EMBO J.* **17,** 6124–6134 (1998).
18. Wyttenbach, A. *et al.* Effects of heat shock, heat shock protein 40 (HDJ-2), and proteasome inhibition on protein aggregation in cellular models of Huntington's disease. *Proc. Natl Acad. Sci. USA* **97,** 2898–2903 (2000).
19. Chai, Y., Koppenhafer, S. L., Bonini, N. M. & Paulson, H. L. Analysis of the role of heat shock protein (Hsp) molecular chaperones in polyglutamine disease. *J. Neurosci.* **19,** 10338–10347 (1999).
20. Kazemi-Esfarjani, P. & Benzer, S. Genetic suppression of polyglutamine toxicity in *Drosophila*. *Science* **287,** 1837–1840 (2000).
21. Hazeki, N., Tukamoto, T., Goto, J. & Kanazawa, I. Formic acid dissolves aggregates of an N-terminal huntingtin fragment containing an expanded polyglutamine tract: applying to quantification of protein components of the aggregates. *Biochem. Biophys. Res. Commun.* **277,** 386–393 (2000).
22. Moulder, K. L., Onodera, O., Burke, J. R., Strittmatter, W. J. & Johnson, E. M. Jr Generation of neuronal intranuclear inclusions by polyglutamine–GFP: analysis of inclusion clearance and toxicity as a function of polyglutamine length. *J. Neurosci.* **19,** 705–715 (1999).
23. Cummings, C. J. *et al.* Chaperone suppression of aggregation and altered subcellular proteasome localization imply protein misfolding in SCA1. *Nature Genet.* **19,** 148–154 (1998).
24. Bence, N. F., Sampat, R. M. & Kopito, R. R. Impairment of the ubiquitin-proteasome system by protein aggregation. *Science* **292,** 1552–1555 (2001).
25. Hurlbert, M. S. *et al.* Mice transgenic for an expanded CAG repeat in the Huntington's disease gene develop diabetes. *Diabetes* **48,** 649–651 (1999).
26. Farrer, L. A. Diabetes mellitus in Huntington disease. *Clin. Genet.* **27,** 62–67 (1985).
27. Li, H., Li, S. H., Johnston, H., Shelbourne, P. F. & Li, X. J. Amino-terminal fragments of mutant huntingtin show selective accumulation in striatal neurons and synaptic toxicity. *Nature Genet.* **25,** 385–389 (2000).
28. DiFiglia, M. *et al.* Aggregation of huntingtin in neuronal intranuclear inclusions and dystrophic neurites in brain. *Science* **277,** 1990–1993 (1997).
29. Onodera, O. *et al.* Oligomerization of expanded-polyglutamine domain fluorescent fusion proteins in cultured mammalian cells. *Biochem. Biophys. Res. Commun.* **238,** 599–605 (1997).
30. Carter, R. J. *et al.* Characterization of progressive motor deficits in mice transgenic for the human Huntington's disease mutation. *J. Neurosci.* **19,** 3248–3257 (1999).

Supplementary Information accompanies the paper on *Nature*'s website (http://www.nature.com/nature).

Acknowledgements We thank E. Signer, S. Lokey, M. Kirschner, N. Ayad, M. Kobori, O.Gozani, L. Yoo, R. Sanchez-Olea, A. Degterev and R. King for comments; T. Mitchison for advice; M. Takeuchi for technical assistance; and X.-J. Li, A. Kazantsev and C. Cepko for reagents. This work was supported in part by grants from the Hereditary Disease Foundation and the NIH (to J.Y.).

Competing interests statement The authors declare that they have no competing financial interests.

Correspondence and requests for materials should be addressed to J.Y. (e-mail: Junying_Yuan@hms.harvard.edu).

A role for *Drosophila* LKB1 in anterior–posterior axis formation and epithelial polarity

Sophie G. Martin & Daniel St Johnston

The Wellcome Trust/Cancer Research UK Institute and Department of Genetics, University of Cambridge, Tennis Court Road, Cambridge CB2 1QR, UK

The PAR-4 and PAR-1 kinases are necessary for the formation of the anterior–posterior (A–P) axis in *Caenorhabditis elegans*[1–3]. PAR-1 is also required for A–P axis determination in *Drosophila*[4,5]. Here we show that the *Drosophila par-4* homologue, *lkb1*, is required for the early A–P polarity of the oocyte, and for the repolarization of the oocyte cytoskeleton that defines the embryonic A–P axis. LKB1 is phosphorylated by PAR-1 *in vitro*, and overexpression of LKB1 partially rescues the *par-1* phenotype. These two kinases therefore function in a conserved pathway for axis formation in flies and worms. *lkb1* mutant clones also disrupt apical–basal epithelial polarity, suggesting a general role in cell polarization. The human homologue, LKB1, is mutated in Peutz–Jeghers syndrome[6,7] and is regulated by prenylation and by phosphorylation by protein kinase A[8,9]. We show that protein kinase A phosphorylates *Drosophila* LKB1 on a conserved site that is important for its activity. Thus, *Drosophila* and human LKB1 may be functional homologues, suggesting that loss of cell polarity may contribute to tumour formation in individuals with Peutz–Jeghers syndrome.

The A–P axis of *Drosophila* is specified during oogenesis when a signal from the posterior follicle cells induces the formation of a polarized oocyte microtubule cytoskeleton, in which most minus ends are nucleated from the anterior cortex, with the plus ends extending towards the posterior pole[10]. These polarized microtubules direct both the localization of *bicoid* messenger RNA to the anterior of the oocyte to specify where the head and thorax will develop, and the transport of *oskar* mRNA to the posterior, where it induces the formation of polar granules that contain the abdominal and germline determinants[10].

To identify other genes required for formation of the A–P axis, we carried out a genetic screen in germline clones for mutants that disrupt the localization of Staufen tagged with green fluorescent protein (GFP), which colocalizes with *bicoid* and *oskar* mRNAs[11]. Mutants in one lethal complementation group of two alleles abolish the posterior localization of both Staufen and *oskar* mRNA in 80–90% of oocytes ($n = 207$; Fig. 1a, b, i, j). In over 40% of mutant oocytes, both *bicoid* and *K10* mRNAs are detected around the whole oocyte cortex, rather than only at the anterior pole ($n = 309$; Fig. 1c, d, and data not shown). In contrast to wild-type oocytes, which have an anterior-to-posterior gradient of microtubules, mutant oocytes have a high density of microtubules all around the cortex, with the lowest concentration in the centre (Fig. 1e, f). Kinesin–β-galactosidase, a microtubule plus-end marker[12], also fails to concentrate at the posterior of the oocyte and accumulates instead in the centre (98%, $n = 80$; Fig. 1g–j). Thus, these mutants disrupt *bicoid* and *oskar* mRNA localization by preventing the A–P polarization of the microtubules.

Using a mapping strategy based on single-nucleotide polymorphisms, we located this complementation group to a 46-kilobase (kb) fragment in 87F (ref. 13). The sequencing of candidate genes showed that both alleles contain lesions in CG9374, which are predicted to be null mutations (Fig. 2a). A genomic rescue construct rescues both lethality and localization of *oskar* mRNA to the posterior of the oocyte, confirming that these phenotypes are caused by mutations in this gene. CG9374 encodes a serine/threonine kinase with homology to *C. elegans* PAR-4 (ref. 2), a kinase involved in the localization of P granules to the posterior of the one-cell zygote[1], and to the human tumour-suppressor LKB1 (refs 6, 7, and Fig. 2a). Given the stronger homology to the latter, we named the *Drosophila* gene *lkb1*.

Hypomorphic mutants in *Drosophila par-1* show defects in the polarization of the oocyte microtubule cytoskeleton and in the localization of *bicoid* and *oskar* mRNA that are very similar to the defects of *lkb1* mutants[4,5,14]. The PAR-1 kinase is also required much earlier in oogenesis for the determination of the oocyte. The oocyte is selected from a cyst of 16 germline cells in the germarium and forms a microtubule-organizing centre, which directs the microtubule-dependent localization of oocyte-specific factors, such as ORB, to this cell[15]. The microtubule-organizing centre then moves from the anterior to the posterior of the oocyte in region 3, the most posterior region of the germarium, and oocyte-specific factors accumulate posteriorly[16]. This anterior-to-posterior switch is disrupted in *par-1* null mutants, and the oocyte exits meiosis and becomes a nurse cell[16,17].

To study the role of *lkb1* in this process, we induced mutant germline clones marked by the loss of GFP. ORB still accumulates in the presumptive oocyte in *lkb1* cysts but often fails to move to the posterior in region 3; instead, it disperses throughout the cyst as the oocyte exits meiosis and adopts the nurse cell fate (Fig. 1k, l). Thus, *lkb1* and *par-1* share very similar phenotypes in both oocyte determination and polarization, suggesting that they function together. Because the penetrance of the early *lkb1* phenotype increases with age (67% ($n = 68$) of mutant clones in 5-day-old females, rising to 85% ($n = 73$) after 12 d), wild-type LKB1 activity seems to perdure for several days after the clones are induced, and

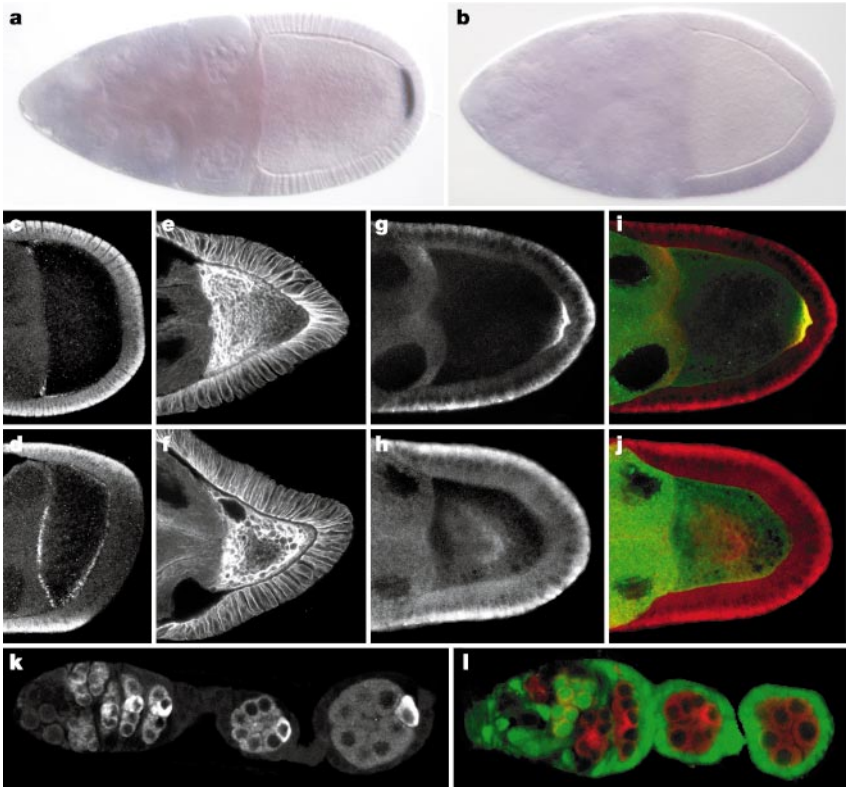

Figure 1 *lkb1* mutants affect oocyte polarity. **a**, **c**, **e**, **g**, **i**, **k**, Wild type. **b**, **d**, **f**, **h**, **j**, **l**, Mutant germline clones. Both alleles have an identical phenotype and therefore only one allele is shown (4A4-2: **b**, **d**, **f**, **l**; 4B1-11: **h**, **j**). **a**, **b**, *In situ* hybridization for *oskar* mRNA. Staufen and *oskar* mRNA accumulate in the oocyte but fail to localize to the posterior in 80–90% of the cases. The residual posterior localization in 10–20% of the oocytes is probably due to perdurance of the protein, as shown for the oocyte determination phenotype. The resulting embryonic phenotype could not be scored because embryos arrest before cellularization. **c**, **d**, Fluorescent *in situ* hybridization for *bicoid* mRNA. **e**, **f**, α-Tubulin staining. **g**, **h**, Kinesin–β-gal localization, detected with an antibody against β-gal. **i**, **j**, Overlay of kinesin–β-gal (red) and GFP–Staufen (green). Colocalization is shown in yellow. **k**, ORB staining in wild type. **l**, ORB staining (red) in homozygous 4A4-2 clones, marked by the absence of GFP (green). ORB accumulates in the oocyte but fails to relocalize to the posterior. Anterior is to the left, posterior is to the right in all figures.

this presumably accounts for the escapers that show the later oocyte polarity phenotype.

As PAR-1 and LKB1 seem to act in a common pathway, we tested whether either kinase could phosphorylate the other. Although recombinant PAR-1 is not a substrate for LKB1, immunoprecipitated GFP–PAR-1 phosphorylates recombinant LKB1 *in vitro* (Fig. 3a). We found that the phosphorylation site or sites are located in the amino-terminal half of the protein, although we have been unable to map them precisely. We also observed a strong genetic interaction between the two genes. The *oskar* mRNA localization defects in hypomorphic combinations of *par-1* alleles cause loss of abdominal segments in the embryo, which can be strongly enhanced by removing one copy of *lkb1* (Supplementary Fig. 1a). In addition, overexpression of GFP–LKB1 partially rescues the A–P polarity phenotype of $par\text{-}1^{6323}/par\text{-}1^{W3}$, the strongest allelic combination that produces late-stage oocytes. Whereas Staufen localizes to the posterior normally in only 12% of these oocytes, 80% have wild-type amounts of Staufen at the posterior when LKB1 is overexpressed (Supplementary Fig. 1b). This phenotype is not rescued by a kinase-dead form of LKB1 (Supplementary Fig. 2), indicating that this suppression requires kinase activity. By contrast, overexpression of PAR-1 does not rescue the phenotype of *lkb1* mutant germline clones (data not shown). These results are consistent with a model in which LKB1 is a direct target of PAR-1 regulation *in vivo* and functions as a downstream effector in the polarization of the oocyte microtubule cytoskeleton.

A GFP–LKB1 fusion construct under the control of the endogenous promoter rescues both the lethality and oogenesis phenotypes of *lkb1* mutants and is expressed in very low amounts in both the germline and somatic follicle cells of the ovary (Fig. 2c). The highest expression was observed in the germarium, where GFP–LKB1 colocalizes with PAR-1 on the fusome[16,17], a branched membranous organelle that connects the germ cells in a cyst (ref. 15 and Fig. 2d). This localization presumably reflects their common function in early oocyte polarity and determination, because the cell that inherits most fusome is selected to become the oocyte[18]. During the rest of oogenesis, GFP–LKB1 shows a uniform cortical localization in both the germline and the follicle cells (Fig. 2c, f, g). It is enriched in the oocyte from stage 7, when the A–P axis is polarized, and colocalizes with cortical actin, but not with pole plasm components (Fig. 2e).

The centrally located kinase domain of LKB1 has 44% and 66% amino-acid identity with PAR-4 and human LKB1, respectively, but the amino- and carboxy-terminal regions are not well conserved (Fig. 2a). *Drosophila* and human LKB1 share a C-terminal prenylation motif (Fig. 2b), however, and the latter is prenylated *in vivo*, which is necessary for its localization to the plasma membrane[8,9]. Mutation of the prenyl-acceptor cysteine to alanine (C537A) in *Drosophila* GFP–LKB1 results in a cytoplasmic accumulation of the protein, showing that *Drosophila* LKB1 is targeted to the cell cortex through prenylation (100%, $n = 71$; Fig. 2g, h). This cortical localization is essential for LKB1 function, because UAS–GFP–$LKB1^{C537A}$ does not rescue the *lkb1* phenotype when expressed in near-endogenous amounts (Fig. 3c). This construct can, however, partially rescue the posterior localization of Staufen when it is expressed in tenfold higher amounts (Fig. 3d). In agreement with this observation, the $LKB1^{C537A}$ mutant shows a weak residual membrane localization, which may be sufficient to mediate LKB1 function when overexpressed. Thus, cortical localization is important for LKB1 activity, consistent with its role in organizing microtubules along the lateral and posterior cortex.

Drosophila LKB1 also has a conserved RKLS consensus phosphorylation site near its C terminus (Fig. 2b). In mammalian LKB1, this site is phosphorylated *in vitro* and *in vivo* by protein kinase A (PKA) and is required for its ability to suppress cell growth in culture[8,9]. Like its vertebrate counterparts, *Drosophila* LKB1 is phosphorylated in a PKA-dependent manner. Coexpression of wild-type LKB1 and PKA in S2 cells induces a phosphatase-sensitive mobility shift of LKB1 on western blots, which is abolished when serine 535 is mutated to alanine (Fig. 3b). To assay the significance of phosphorylation of this conserved site, we generated transgenes in which the serine was mutated to either alanine (S535A) to prevent phosphorylation, or to glutamic acid (S535E) to mimic the presence

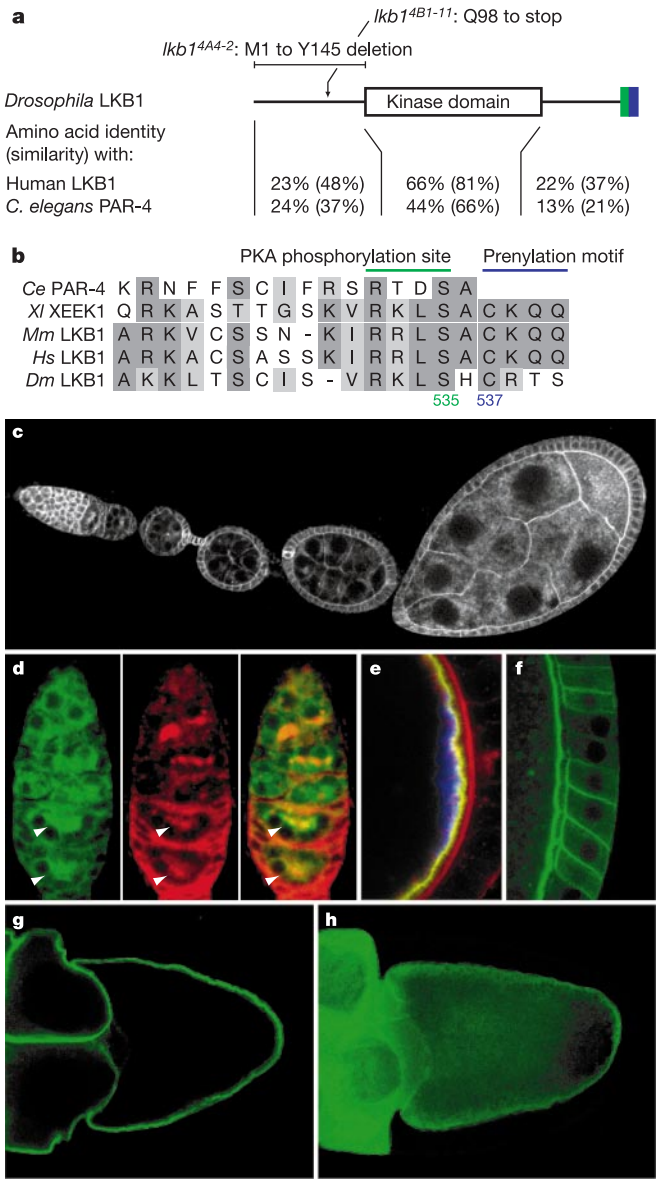

Figure 2 Conservation and localization of LKB1. **a**, $lkb1^{4A4\text{-}2}$ contains a 589-bp deletion (associated with a 12-bp insertion) removing 150 bp of the 5′ untranslated region, the start codon and the beginning of the ORF. $lkb1^{4B1\text{-}11}$ contains a nonsense mutation at amino acid 98. The conserved kinase, phosphorylation (green) and prenylation (blue) domains are indicated. **b**, Alignment of the C termini of LKB1 homologues, showing the phosphorylation (S535) and prenylation (C537) motifs conserved between *Drosophila* and human LKB1. **c**, Expression of the GFP–LKB1 genomic transgene showing endogenous expression of *lkb1*. Because expression is very low, this image was taken at 100% laser power and the diffuse cytoplasmic staining is background. **d**, GFP–LKB1 (green) and PAR-1 (red) colocalize on the fusome in regions 2b and 3 of the germarium (arrowheads). **e**, GFP–LKB1 (green) colocalizes with actin (red) but not with Staufen (blue) in stage-10 oocytes. UAS–GFP–LKB1 was driven by matα4–GAL4–VP16. **f**, GFP–LKB1 localizes cortically in follicle cells. UAS–GFP–LKB1 was driven by da–GAL4. **g**, Expression of wild-type GFP–LKB1. **h**, Expression of GFP–$LKB1^{C537A}$, which cannot be prenylated. In **f** and **g**, both transgenes were expressed at similar levels, driven by matα4–GAL4–VP16.

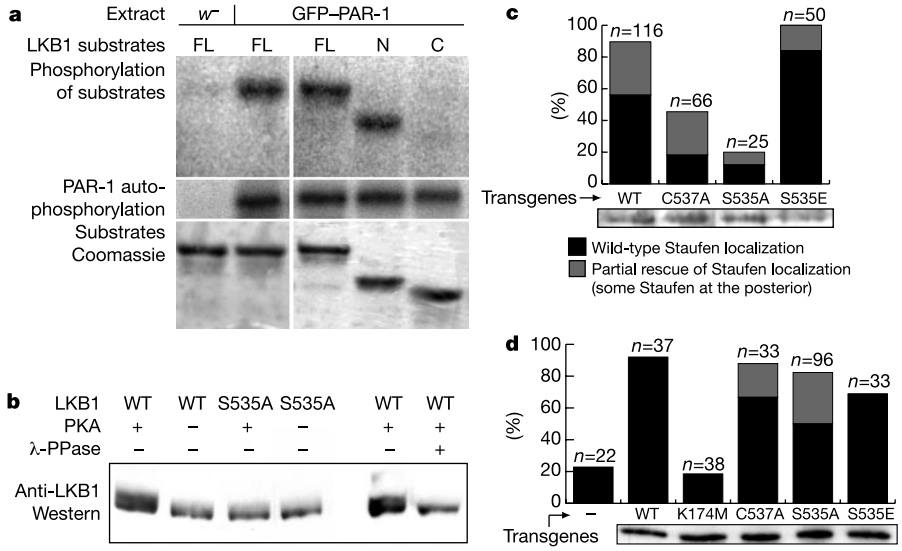

Figure 3 Analysis of LKB1 regulation. **a**, Immunoprecipitated GFP–PAR-1 phosphorylates the N-terminal half of recombinant LKB1 *in vitro*. As a control, immunoprecipitation was also carried out with a w^- extract. PAR-1 autophosphorylation shows equal levels of PAR-1 activity. FL, LKB1 full length; C, C terminus; N, N terminus. **b**, Western blot of extracts of S2 cells transfected with LKB1 and PKA as indicated and detected with antibodies against LKB1. Coexpression of LKB1 and PKA induces a mobility shift in LKB1, which is dependent on S535 and abolished by phosphatase treatment. **c**, Rescue of the posterior localization of Staufen in $lkb1^{4A4\text{-}2}/lkb1^{4B1\text{-}11}$ flies by expression of UAS–GFP–LKB1. Transgenes were expressed with *arm*–GAL4, and $lkb1^{4A4\text{-}2}/lkb1^{4B1\text{-}11}$ flies were recovered expressing low levels of *lkb1* in the germ line. GFP–LKB1^{C537A} and GFP–LKB1^{S535A} transgenes show impaired function; by contrast, GFP–LKB1^{S535E} rescues more efficiently than wild-type. Western blot with antibodies against GFP shows that all transgenes are expressed in similar quantities. For S535A, only egg chambers with wild-type morphology were scored (see Fig. 4). **d**, Overexpression of wild-type and mutant transgenes with matα4–GAL4–VP16 in $lkb1^{4A4-2}$ germline clones. The kinase-dead mutant GFP–LKB1^{K174M} (see Supplementary Fig. 2) is unable to rescue, whereas the phosphorylation (GFP–LKB1^{S535A}) and prenylation (GFP–LKB1^{C537A}) mutants rescue LKB1 function when overexpressed. Western blot with antibodies against GFP shows that all transgenes are expressed in similar amounts, about tenfold more than endogenous protein.

of a charged phosphate group. Expression of the transgenes with *arm*–GAL4 allows the recovery of *lkb1* mutant flies expressing low amounts of either wild-type or mutant proteins in the germ line[19]. GFP–LKB1^{S535A} does not rescue the localization of Staufen to the posterior of the oocyte, whereas GFP–LKB1^{S535E} rescues even more efficiently than the wild-type control, strongly suggesting that LKB1 is positively regulated by phosphorylation at this site (Fig. 3c). Because S535 is phosphorylated by PKA *in vivo* and PKA is required in the germ line to polarize the oocyte[20], we speculate that PKA regulates *Drosophila* LKB1 in the germ line. Additional signals must regulate LKB1, however, because the lack of phosphorylation on S535 does not abolish LKB1 activity completely. Tenfold overexpression of S535A in *lkb1* germline clones partially rescues the localization of Staufen to the posterior of the oocyte, albeit less efficiently than the wild-type transgene, whereas a kinase-dead version (K174M) shows no rescuing activity on overexpression

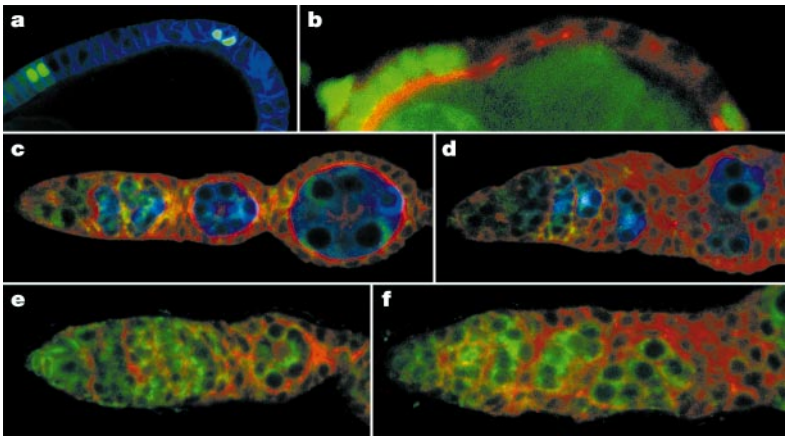

Figure 4 *lkb1* is required for epithelial polarity. **a**, **b**, $lkb1^{4A4-2}$ follicle cell clones marked by the absence of GFP (green) and stained for α-spectrin (**a**, blue) and aPKC (**b**, red). **c**, **d**, GFP–LKB1^{S535E} (**c**, green) but not GFP–LKB1^{S535A} (**d**, green) rescues the apical localization of aPKC (red) in the follicular epithelium. ORB (blue) stains the germ line. **e**, **f**, Similarly, wild-type GFP–LKB1 (**e**, green) but not GFP–LKB1^{S535A} (**f**, green) rescues the apical localization of Armadillo (red), a component of adherens junctions. Most ovarioles expressing GFP–LKB1^{S535A} show aberrant morphology of the germarium (**d**, **f**), a phenotype that is also observed with large somatic *lkb1* clones (not shown). In **c**–**f**, transgenes were driven by *arm*–GAL4 in $lkb1^{4A4-2}/lkb1^{4B1-11}$ flies. LKB1 has been implicated in apoptosis and cell-cycle control[23], but the polarity phenotype observed was not a consequence of cell death or overproliferation because TUNEL assay and phosphohistone H3 staining failed to detect more apoptotic or mitotic cells in mutant clones than in their wild-type neighbours (not shown). Thus, *lkb1* seems to have a specific role in the polarity of epithelial cells.

(Fig. 3d and Supplementary Fig. 2). Thus, LKB1 may be regulated by both PAR-1 and PKA, and may function to integrate the two signalling pathways during the polarization of the oocyte.

Follicle cell clones mutant for *lkb1* also show a defect in polarity. In severely affected clones, the follicular monolayer is disorganized, with mutant cells rounding up and sorting out of the epithelium (Fig. 4a). Morphologically wild-type clones show defects in the apical localization of atypical protein kinase C (aPKC) and Armadillo, which become either diffuse or ectopically localized along lateral membranes (Fig. 4b). In less severely affected cells, the apical localization is discontinuous. These phenotypes are penetrant in large stem-cell clones but not in small clones, indicating that LKB1 activity perdures. Expression of the wild-type or S535E transgenes with *arm*–GAL4 in *lkb1* mutants rescues these follicle cell phenotypes, whereas expression of S535A rescues lethality but gives rise to a completely disorganized follicular epithelium, in which most cells appear unpolarized (Fig. 4c–f). Thus, LKB1 is required for cell polarity in the germ line and the follicle cells, and is probably regulated by phosphorylation on the conserved C-terminal serine in both processes.

In *Drosophila*, *par-1* and *lkb1*, the homologue of *C. elegans par-4*, show very similar phenotypes[4,5]. In addition, LKB1 is an *in vitro* substrate for PAR-1 and can suppress the polarity phenotype of *par-1* mutants when overexpressed. These results suggest that LKB1 functions downstream of PAR-1. This conclusion is consistent with genetic data in *C. elegans* that show that *par-4* mutants display only a subset of the *par-1* A–P polarity phenotypes. Notably, mutants in *par-4* and *par-1*, but not in other *par* genes, show a disappearance of P granules in the one-cell zygote[1]. Thus, LKB1 and PAR-1 function in a conserved pathway that is required for the polarization of the A–P axis in both worms and flies.

Drosophila LKB1 is closely related to human LKB1, and conserved prenylation and PKA phosphorylation sites are essential for the *in vivo* function of both proteins, indicating that the two are likely to be functional homologues. Mutants in LKB1 cause Peutz–Jeghers syndrome[6,7], which is characterized by the formation of intestinal polyps and a high incidence of adeno-carcinomas (tumours of epithelial origin)[21]. In addition, mutations in *lkb1* have been identified in several sporadic epithelial cancers[22]. The role of LKB1 as a tumour suppressor is not well understood, however, and LKB1 has been proposed to regulate apoptosis, the cell cycle or angiogenesis[23]. In addition, LKB1 seems to function in a context-dependent manner that is different from classical tumour-suppressor genes such as *ras* or *p53* (ref. 24). Given that *Drosophila lkb1* is required to polarize the epithelial follicle cells, we propose the alternative model that loss of LKB1 leads to polyp and tumour formation by disrupting epithelial polarity. □

Methods

Fly strains

We used the following strains: $par\text{-}1^{W3}$, $par\text{-}1^{6323}$ and $par\text{-}1^{6821}$ (ref. 4). $lkb1^{4A4\text{-}2}$ and $lkb1^{4B1\text{-}11}$ were induced by ethyl methyl sulphonate (EMS) on the FRT82B chromosome and identified on the basis of their failure to localize GFP–Staufen to the posterior of the oocyte (S.G.M., V. Leclerc, K. Litière and D.S.J., manuscript in preparation). The FLP–FRT system was used to induce clones[25], in combination with either ovo^{D1} (ref. 26) or GFP (a gift from S. Luschnig) for clone selection. GFP–Staufen was expressed under the control of the matα4–tubulin promoter. The kinesin–β-galactosidase transgene[12] was mobilized to obtain an insertion on the first chromosome. For rescue of lethality and low expression in the ovaries, we used *arm*GAL4 (ref. 27). matα4–tubulin–GAL4–VP16 was used for overexpression in the germ line. We used da–GAL4 to study the localization of GFP–LKB1 in somatic follicle cells[28].

Molecular biology

The genomic rescue construct contains the DNA between the two genes adjacent to *lkb1*. GFP was inserted in-frame upstream of the *lkb1* open reading frame (ORF CG9374) to create the genomic GFP–LKB1 construct. Inducible GFP–LKB1 transgenes were obtained by inserting the 3.6-kb *lkb1* transcription unit, amplified from the genomic GFP construct, into the UASp vector[19]. Mutant versions were generated using *in vitro* site-directed mutagenesis based on polymerase chain reaction (PCR) and sequenced. MBP–lkb1 plasmids were obtained by inserting *lkb1* fragments amplified from GH14740 (BDGP; the ORF is identical to that available under GenBank accession number AY069241) into pMal (NEB) in-frame downstream of MBP. LKB1N includes amino-acids 1–301 of the CG9374 protein, and LKB1C includes amino acids 272–540. For expression in S2 cells, we cloned PKA in pMT–DEST48 in-frame with the His_6–V5 epitope at the C terminus using Gateway Technology (Invitrogen). LKB1 was also cloned into pMT–DEST48 with the inclusion of a stop codon, so that LKB1 was untagged.

Kinase assay

Ovaries from either w^- or *matα4–GFP–PAR-1*^{N1S} (ref. 16) flies were homogenized in 150 mM NaCl, 50 mM HEPES (pH 7.2), 0.5 mM dithiothreitol and 1 μM microcystin-LR, supplemented with protease inhibitors (Roche). We carried out immunoprecipitations with affinity-purified polyclonal antibodies against GFP bound to magnetic Dynabeads (Dynal). Kinase buffer (50 mM HEPES (pH 7.4), 1 mM EDTA, 5% glycerol, 150 mM NaCl, 10 mM $MgCl_2$ and 10 mM $MnCl_2$) and substrate (2 μM) were mixed directly with the beads and the reaction was started by adding [γ-^{32}P]ATP. After a 20-min incubation at 30 °C, the reaction was stopped by adding Laemmli buffer and analysed by SDS–PAGE. ^{32}P incorporation was detected by a phosphorimager. Substrates were expressed as maltose-binding protein (MBP) fusion proteins in bacteria, and purified over amylose columns (NEB). The same procedure, without added substrate, was used for autophosphorylation assays, using ovarian extracts from flies carrying matα4–GAL4–VP16 and UASp–GFP–LKB1 transgenes.

Cell culture and phosphatase treatment

S2 cells were maintained in Schneider's medium supplemented with 5% fetal calf serum (Sigma). We transfected 10^6 cells per ml with 1 μg of total DNA (0.2 μg of LKB1 and either 0.8 μg of PKA or 0.8 μg of empty pMT–DEST48 vector) with FuGENE 6 (Roche). After 24 h, the culture medium was removed and fresh medium containing 200 μM $CuSO_4$ was added to induce expression of the metallothionein promoter. We collected the cells 24 h later, and resuspended them in RIPA buffer (150 mM NaCl, 1% Nonidet P-40, 0.5% deoxycholate, 0.1% SDS, 50 mM Tris pH 8.0, 0.4 mM EDTA, 10% glycerol and protease inhibitor cocktail (Roche)). Treatment with λ-phosphatase (NEB) was carried out at 30 °C for 30 min and stopped by the addition of Laemmli buffer.

Immunostaining and *in situ* hybridization

We carried out immunostaining according to standard procedures using the following antibodies: a rabbit polyclonal against Staufen (ref. 11; used at 1:5,000 dilution), a rabbit polyclonal against PAR-1 (ref. 29; 1:1,250), a mouse monoclonal against β-gal (JIE7; 1:400), a mouse monoclonal against ORB (6H4 and 4H8; 1:500), a mouse monoclonal against Armadillo (7A1; 1:200) and a mouse monoclonal against α-spectrin (3A9; 1:1000) from DSHB; a rabbit polyclonal against aPKC (Santa Cruz; 1:500); and a rabbit polyclonal against phosphohistone H3 (Upstate Biotechnology; 1:1,000). Texas-red-, fluorescein isothiocyanate (FITC)- and Cy5-conjugated secondary antibodies (Molecular Probes) were used at a 1:200 dilution. For microtubule staining, we fixed samples for 10 min with 8% paraformaldehyde in fixation buffer[30] and stained them with a FITC-conjugated monoclonal antibody against α-tubulin (Sigma; 1:400). Apoptag Red (Intergen) was used for TdT-mediated dUTP nick end labelling (TUNEL) assays. *In situ* hybridizations were carried out using RNA probes labelled with digoxygenin-UTP (Roche). For fluorescent detection, a secondary polyclonal sheep antibody against DIG (Roche; 1:5,000) and a tertiary Cy3-conjugated donkey antibody against sheep IgG (Jackson Immunoresearch; 1:200) were used. Immunohistochemical detection was done with alkaline-phosphatase-conjugated antibodies against DIG (Roche; 1:5,000). We raised LKB1 antibodies against MBP–LKB1N in rabbits (Eurogentech) and affinity-purified them.

Received 19 June; accepted 6 November 2002; doi:10.1038/nature01296.

1. Kemphues, K. J., Priess, J. R., Morton, D. G. & Cheng, N. S. Identification of genes required for cytoplasmic localization in early *C. elegans* embryos. *Cell* **52,** 311–320 (1988).
2. Watts, J. L., Morton, D. G., Bestman, J. & Kemphues, K. J. The *C. elegans par-4* gene encodes a putative serine–threonine kinase required for establishing embryonic asymmetry. *Development* **127,** 1467–1475 (2000).
3. Guo, S. & Kemphues, K. J. *par-1*, a gene required for establishing polarity in *C. elegans* embryos, encodes a putative Ser/Thr kinase that is asymmetrically distributed. *Cell* **81,** 611–620 (1995).
4. Shulman, J. M., Benton, R. & St Johnston, D. The *Drosophila* homolog of *C. elegans* PAR-1 organizes the oocyte cytoskeleton and directs oskar mRNA localization to the posterior pole. *Cell* **101,** 377–388 (2000).
5. Tomancak, P. *et al.* A *Drosophila melanogaster* homologue of *Caenorhabditis elegans par-1* acts at an early step in embryonic-axis formation. *Nature Cell Biol.* **2,** 458–460 (2000).
6. Hemminki, A. *et al.* A serine/threonine kinase gene defective in Peutz–Jeghers syndrome. *Nature* **391,** 184–187 (1998).
7. Jenne, D. E. *et al.* Peutz-Jeghers syndrome is caused by mutations in a novel serine threonine kinase. *Nature Genet.* **18,** 38–43 (1998).
8. Collins, S. P., Reoma, J. L., Gamm, D. M. & Uhler, M. D. LKB1, a novel serine/threonine protein kinase and potential tumour suppressor, is phosphorylated by cAMP-dependent protein kinase (PKA) and prenylated *in vivo*. *Biochem. J.* **345,** 673–680 (2000).
9. Sapkota, G. P. *et al.* Phosphorylation of the protein kinase mutated in Peutz–Jeghers cancer syndrome, LKB1/STK11, at Ser431 by $p90^{RSK}$ and cAMP-dependent protein kinase, but not its farnesylation at Cys433, is essential for LKB1 to suppress cell growth. *J. Biol. Chem.* **276,** 19469–19482 (2001).
10. van Eeden, F. & St Johnston, D. The polarisation of the anterior–posterior and dorsal–ventral axes during *Drosophila* oogenesis. *Curr. Opin. Genet. Dev.* **9,** 396–404 (1999).
11. St Johnston, D., Beuchle, D. & Nüsslein-Volhard, C. *Staufen*, a gene required to localize maternal RNAs in the *Drosophila* egg. *Cell* **66,** 51–63 (1991).
12. Clark, I., Giniger, E., Ruohola-Baker, H., Jan, L. Y. & Jan, Y. L. Transient posterior localization of a kinesin fusion protein reflects anteroposterior polarity of the *Drosophila* oocyte. *Curr. Biol.* **4,** 289–300 (1994).

13. Martin, S. G., Dobi, K. C. & St Johnston, D. A rapid method to map mutations in *Drosophila*. *Genome Biol.* **2,** research0036.1–12 (2001).
14. Benton, R., Palacios, I. M. & St Johnston, D. *Drosophila* 14–3–3/PAR-5 is an essential mediator of PAR-1 function in axis formation. *Dev. Cell* **3,** 659–671 (2002).
15. Spradling, A. *The Development of Drosophila melanogaster* (eds Bate, M. & Martinez-Arias, A.) 1–70 (Cold Spring Harbor Laboratory Press, Cold Spring Harbor, New York, 1993).
16. Huynh, J. R., Shulman, J. M., Benton, R. & St Johnston, D. PAR-1 is required for the maintenance of oocyte fate in *Drosophila*. *Development* **128,** 1201–1209 (2001).
17. Cox, D. N., Lu, B., Sun, T. Q., Williams, L. T. & Jan, Y. N. *Drosophila par-1* is required for oocyte differentiation and microtubule organization. *Curr. Biol.* **11,** 75–87 (2001).
18. de Cuevas, M. & Spradling, A. C. Morphogenesis of the *Drosophila* fusome and its implications for oocyte specification. *Development* **125,** 2781–2789 (1998).
19. Rorth, P. Gal4 in the *Drosophila* female germline. *Mech. Dev.* **78,** 113–118 (1998).
20. Lane, M. E. & Kalderon, D. RNA localization along the anteroposterior axis of the *Drosophila* oocyte requires PKA-mediated signal transduction to direct normal microtubule organization. *Genes Dev.* **8,** 2986–2995 (1994).
21. Hemminki, A. The molecular basis and clinical aspects of Peutz–Jeghers syndrome. *Cell. Mol. Life Sci.* **55,** 735–750 (1999).
22. Sanchez-Cespedes, M. *et al.* Inactivation of LKB1/STK11 is a common event in adenocarcinomas of the lung. *Cancer Res.* **62,** 3659–3662 (2002).
23. Yoo, L. I., Chung, D. C. & Yuan, J. LKB1—a master tumour suppressor of the small intestine and beyond. *Nature Rev. Cancer* **2,** 529–535 (2002).
24. Bardeesy, N. *et al.* Loss of the Lkb1 tumour suppressor provokes intestinal polyposis but resistance to transformation. *Nature* **419,** 162–167 (2002).
25. Xu, T. & Rubin, G. M. Analysis of genetic mosaics in developing and adult *Drosophila* tissues. *Development* **117,** 1223–1237 (1993).
26. Chou, T. B. & Perrimon, N. The autosomal FLP–DFS technique for generating germline mosaics in *Drosophila melanogaster*. *Genetics* **144,** 1673–1679 (1996).
27. Sanson, B., White, P. & Vincent, J. P. Uncoupling cadherin-based adhesion from wingless signalling in *Drosophila*. *Nature* **383,** 627–630 (1996).
28. Wodarz, A., Hinz, U., Engelbert, M. & Knust, E. Expression of crumbs confers apical character on plasma membrane domains of ectodermal epithelia of *Drosophila*. *Cell* **82,** 67–76 (1995).
29. Sun, T. Q. *et al.* PAR-1 is a Dishevelled-associated kinase and a positive regulator of Wnt signalling. *Nature Cell Biol.* **3,** 628–636 (2001).
30. Theurkauf, W. *Drosophila melanogaster: Practical Uses in Cell and Molecular Biology* (eds Goldstein, L. & Fyrberg, E.) 489–506 (Academic, London, 1994).

Supplementary Information accompanies the paper on *Nature*'s website (http://www.nature.com/nature).

Acknowledgements We thank M. Pal for fly injection; K. Litière for generating the kinesin–β-gal line; I. Palacios, B. Sanson, A. Wodarz and the Developmental Studies Hybridoma Bank for strains and antibodies; and J. Rouse, N. Lowe, J. Raff and R. Benton for advice and discussion. S.G.M. was supported by the Swiss National Science Foundation and D.StJ. by the Wellcome Trust.

Competing interests statement The authors declare that they have no competing financial interests.

Correspondence and requests for materials should be addressed to D.StJ. (e-mail: ds139@mole.bio.cam.ac.uk).

Nicotinic acetylcholine receptor α7 subunit is an essential regulator of inflammation

Hong Wang*, Man Yu*, Mahendar Ochani*, Carol Ann Amella*, Mahira Tanovic*, Seenu Susarla*, Jian Hua Li*, Haichao Wang*, Huan Yang*, Luis Ulloa*, Yousef Al-Abed†, Christopher J. Czura* & Kevin J. Tracey*

** Laboratory of Biomedical Science, † Laboratory of Medicinal Chemistry, North Shore Long Island Jewish Research Institute, 350 Community Drive, Manhasset, New York 11030, USA*

Excessive inflammation and tumour-necrosis factor (TNF) synthesis cause morbidity and mortality in diverse human diseases including endotoxaemia, sepsis, rheumatoid arthritis and inflammatory bowel disease[1–4]. Highly conserved, endogenous mechanisms normally regulate the magnitude of innate immune responses and prevent excessive inflammation. The nervous system, through the vagus nerve, can inhibit significantly and rapidly the release of macrophage TNF, and attenuate systemic inflammatory responses[5–7]. This physiological mechanism, termed the 'cholinergic anti-inflammatory pathway'[5] has major implications in immunology and in therapeutics; however, the identity of the essential macrophage acetylcholine-mediated (cholinergic) receptor that responds to vagus nerve signals was previously unknown. Here we report that the nicotinic acetylcholine receptor α7 subunit is required for acetylcholine inhibition of macrophage TNF release. Electrical stimulation of the vagus nerve inhibits TNF synthesis in wild-type mice, but fails to inhibit TNF synthesis in α7-deficient mice. Thus, the nicotinic acetylcholine receptor α7 subunit is essential for inhibiting cytokine synthesis by the cholinergic anti-inflammatory pathway.

Nicotinic acetylcholine receptors are a family of ligand-gated, pentameric ion channels. In human, 16 different subunits (α1–7, α9–10, β1–4, δ, ϵ, γ) have been identified that form a large number of homo- and heteropentameric receptors with distinct structural and pharmacological properties[8–10]. The main function of this receptor family is to transmit signals for the neurotransmitter acetylcholine at neuromuscular junctions and in the central and peripheral nervous systems[8–12]. Our previous studies have indicated that acetylcholine inhibits the release of TNF and other cytokines through a post-transcriptional mechanism that is dependent on α-bungarotoxin-sensitive nicotinic receptors on primary human macrophages[5], but the identity of the specific receptor subunit has remained unknown. As a first step towards identifying this macrophage receptor, primary human macrophages were labelled with fluorescein isothiocyanate (FITC)-tagged α-bungarotoxin, a peptide antagonist that binds to a subset of cholinergic receptors[8,9]. Strong binding of α-bungarotoxin was observed on the macrophage surface (Fig. 1a). Nicotine pretreatment markedly reduced the

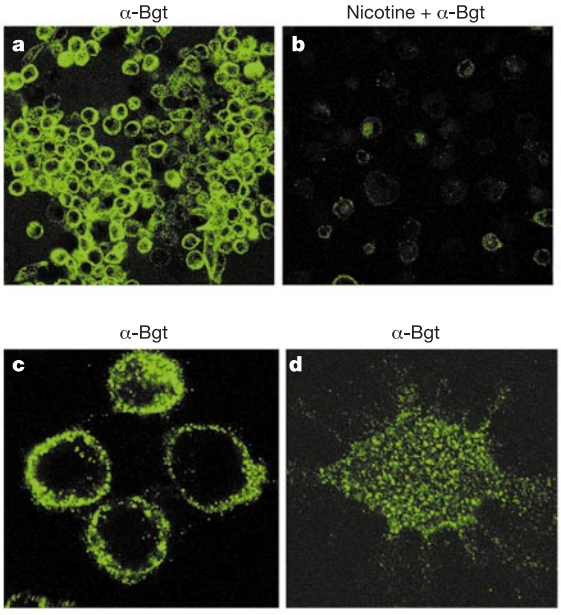

Figure 1 α-Bungarotoxin-binding nicotinic receptors are clustered on the surface of macrophages. Primary human macrophages were stained with fluorescein isothiocyanate (FITC)-labelled α-bungarotoxin (α-Bgt, 1.5 μg ml^{-1}) and viewed by fluorescent confocal microscopy. **a**, Cells were stained with α-bungarotoxin alone. **b**, Nicotine was added to a final concentration of 500μmol before addition of α-bungarotoxin. **c**, **d**, Higher magnification reveals receptor clusters. **c**, Focus planes are on the inside layers close to the middle (three lower cells) or close to the surface (upper cell) of cells. **d**, Focus plane is on the surface of the cell. Magnifications: **a**, **b**, × 50; **c**, × 200; **d**, × 450.

a **maternal-effect embryonic phenotype**

		par-1^{6821}/*par-1*^{W3}		
	wt	*+/TM6B*	*lkb1*$^{4A4-2}$/+	*lkb1*$^{4B1-11}$/+
n^{o} denticle belts	8	4.45	1.66	1.56
n		203	240	174

b **localisation of Staufen**

		par-1^{6323}/*par-1*^{W3}		
	wt	*+/TM2*	*GFP-LKB1/+*	*K174M/+*
wild-type	100%	12%	79%	20%
ectopic localisation	-	73%	19%	68%
diffuse	-	15%	2%	12%
n		84	156	91

Supplementary Figure 1 Genetic interaction between *lkb1* and *par-1*. **a,** Removal of one copy of *lkb1* enhances the *par-1* embryonic phenotype. **b,** LKB1 over-expression partially rescues the posterior localisation of Staufen in *par-1* mutants. GFP-LKB1 or GFP-LKB1^{K174M}, a kinase-dead (see supplementary Figure 2), were over-expressed with mata4-GAL4-VP16 in *par-1*^{6323}/*par-1*^{W3} oocytes. Oocytes in which Staufen was present both at the posterior and in the centre were placed in the “ectopic localisation” class.

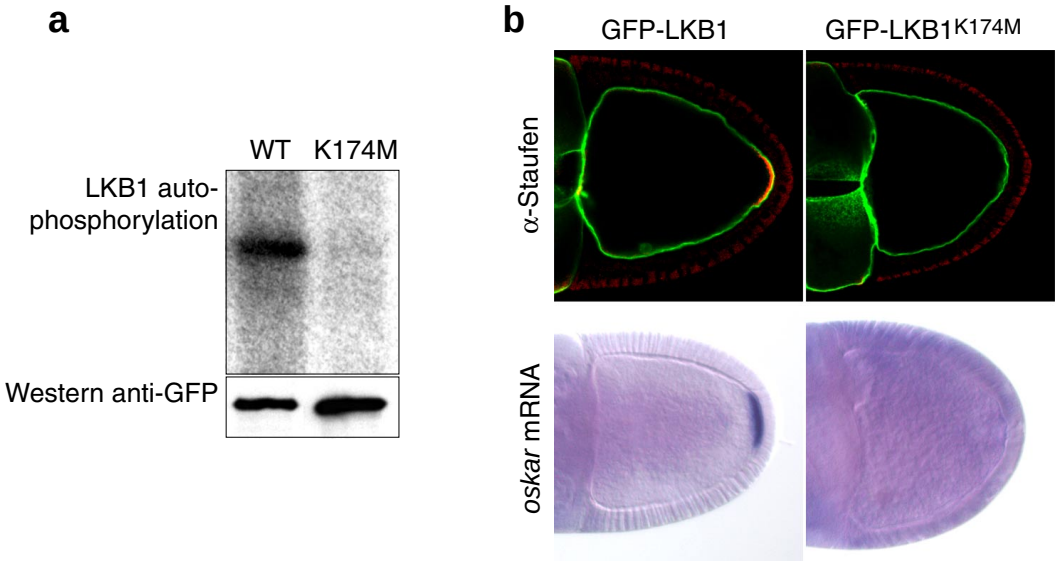

Supplementary Figure 2 Kinase activity is essential for LKB1 function. **a,** Autophosphorylation activity is abolished in immunoprecipitated GFP-LKB1^{K174M}. Upper panel: *in vitro* autophosphorylation assay. Lower panel: anti-GFP Western showing equal loading. **b,** Expression of wildtype GFP-LKB1 (left) but not GFP-LKB1^{K174M} (right) is able to rescue the localisation of Staufen (top, red) and *oskar* mRNA (bottom) to the posterior of the oocyte. GFP-LKB1 is shown in green. Transgenes were driven by mata4-GAL4-VP16 in *lkb1^{4A4-2}* germline clones (see also Fig.3d).